The Astronomical Journal, 138:558–567, 2009 August doi:10.1088/0004-6256/138/2/558

IAC-POP: FINDING THE STAR FORMATION HISTORY OF RESOLVED GALAXIES

Antonio Aparicio[1,2] and Sebastian L. Hidalgo[2]
[1] Departamento de Astrofísica, Universidad de La Laguna, Vía Láctea s/n E38200-La Laguna, Tenerife, Canary Islands, Spain; antapaj@iac.es
[2] Instituto de Astrofísica de Canarias, Vía Láctea s/n E38200-La Laguna, Tenerife, Canary Islands, Spain; shidalgo@iac.es
Received 2007 May 22; accepted 2009 May 17; published 2009 July 7

ABSTRACT

IAC-pop is a code designed to solve the star formation history (SFH) of a complex stellar population system, like a galaxy, from the analysis of the color–magnitude diagram (CMD). It uses a genetic algorithm to minimize a χ^2 merit function comparing the star distributions in the observed CMD and the CMD of a synthetic stellar population. A parameterization of the CMDs is used, which is the main input of the code. In fact, the code can be applied to any problem in which a similar parameterization of an experimental set of data and models can be made. The method's internal consistency and robustness against several error sources, including observational effects, data sampling, and stellar evolution library differences, are tested. It is found that the best stability of the solution and the best way to estimate errors are obtained by several runs of IAC-pop with varying the input data parameterization. The routine *MinnIAC* is used to control this process. IAC-pop is offered for free use and can be downloaded from the site http://iac-star.iac.es/iac-pop. The routine MinnIAC is also offered under request, but support cannot be provided for its use. The only requirement for the use of IAC-pop and MinnIAC is referencing this paper and crediting as indicated in the site.

Key words: galaxies: stellar content – Hertzsprung–Russell (HR) diagram – Local Group – methods: numerical

Online-only material: color figures

1. INTRODUCTION

Galaxies evolve on two main paths: dynamically, including interaction with external systems, and through the process of formation, evolution, and death of stars within them. The latter has the following relevant effects on the galaxy: (1) the evolution of gas content, (2) the chemical enrichment, and (3) the formation of the stellar populations with different properties as the gas from which they form evolves. The star formation history (SFH) is therefore fundamental to understanding the galaxy evolution process.

The color–magnitude diagram (CMD) is, in practice, the best tool to study and derive the SFH of resolved galaxies. Deep enough CMDs display stars born all over the lifetime of the galaxy and are indeed fossil records of the SFH. An approximate, qualitative sketch of the stellar populations present in a galaxy can be done from a quick look at a good CMD. The presence of stars in characteristic evolutionary phases indicates that star formation took place in the system in one or another epoch of its history. For example, the presence of RR-Lyrae stars is indicative of an old, low-metallicity stellar population; a substantial amount of red giant branch (RGB) stars is associated to an intermediate-age to old star formation activity; a well-developed red tail of asymptotic giant branch (AGB) stars shows that intermediate-age to young stars with relatively high metallicity are present in the system, and even a few blue, bright stars as well as H II regions are evidences of a very recent star formation activity.

A higher degree of sophistication is provided by isochrone fitting to significant features of the CMD. Indeed, this method is simple and powerful enough to determine age and metallicity of simple stellar populations as the ones present in star clusters. However, actually deciphering the information contained in a complex CMD and deriving a quantitative, accurate SFH is complicated and requires some relatively sophisticated technique. Although other approaches are possible (see below), the most extended and probably most powerful technique is the one based on synthetic CMD analysis. The standard procedure involves three main ingredients: (1) a CMD ideally reaching the oldest main-sequence turnoffs; (2) one (or several) synthetic CMDs, computed assuming a set of input physical parameters, and (3) a method to derive the SFH from the comparison of the star distributions in observational and synthetic CMDs.

In Aparicio & Gallart (2004), we presented IAC-star, a code for synthetic CMD computation. In short, the algorithm is intended to be as general as possible and allows a variety of inputs for the initial mass function (IMF), star formation rate, metallicity law, and binarity. Stars with age and metallicity following a continuous distribution are computed through interpolation in a stellar evolution library, providing synthetic CMDs with smooth, realistic stellar distributions.

In this paper, we present an algorithm corresponding to ingredient (3), i.e., designed for deriving the SFH from the comparison of observed and synthetic CMDs. Several approaches have been used in the past. Indeed, interest in the process of formation of stellar populations is not new. The early works by Baade (1944) can be considered a starting point. However, the amount of information and results have been largely increased in the last few decades and it is only since relatively recently that we have been able to speak properly about quantitative determinations of complex SFHs. Tosi et al. (1991) used a method based on the comparison of luminosity functions of observed and synthetic CMDs. They were the first to sketch SFHs of nearby galaxies using synthetic CMDs. Bertelli et al. (1992) introduced the R-method, the first to make use of the global morphology and number counts of the distribution of stars in synthetic and observed CMDs to derive the SFH of a galaxy (the LMC). Gallart et al. (1996) used an extended, more complete version of the R-method to study the SFH of the Local Group galaxy NGC 6822. Tolstoy & Saha (1996) used maximum likelihood to find out the synthetic CMD, of a set of them, best reproducing the

observed one. Vergely et al. (2002) presented an inverse method to interpret the CMD in terms of the SFH.

Aparicio et al. (1997) introduced a new approach in which the SFH is derived by linear combination of several simple populations. This method allows a SFH derivation free from initial assumptions about it and has the important advantage of requiring only a single synthetic CMD. The same idea was independently introduced by Dolphin (1997) and also has been applied by Holtzman et al. (1999), who, for the first time, derived the star formation rate (SFR) as a function of time and chemical enrichment law (CEL) simultaneously, making no assumptions about the CEL morphology, by Olsen (1999), by Harris & Zaritsky (2001), and by Rizzi et al. (2003) and has been used in several works of the former authors (e.g., Gallart et al. 1999; Aparicio et al. 2000, 2001; Holtzman et al. 2000; Dolphin 2000a, 2000b; Wyder 2001; Sabbi et al. 2007; Chiosi & Vallenari 2007; see Aparicio 2002 for a review).

The former methods do in general include some kind of parameterization of the CMD. In this short historical overview, we must also mention the contribution by Hernández et al. (1999) as an alternative, nonparametric method for the derivation of SFH of galaxies which make direct use of the information contained in a stellar evolution library and it is not based on synthetic CMDs.

The code we present here is based on the same principle as that used by Aparicio et al. (1997) but makes use of a genetic algorithm (*pikaia*; Charbonneau 1995) for the solution convergence. Applied in the most general way it derives the SFR as a function of both time and metallicity or, from a different point of view, the SFR and the CEL as a function of time of a system from the comparison of its CMD star distribution with the star distribution in a single template synthetic CMD.

The code is made available for free use. It can be downloaded from the Internet site http://iac-star.iac.es/iac-pop with the only requirement of referencing this paper and crediting as indicated in that site. It is worth mentioning that the code is not restricted to the SFH solution only, but to any problem that can be parameterized in a similar way. The present paper should be considered as the reference for the code. This paper is a complement of our previous one presenting IAC-star, the code for synthetic CMD computation (Aparicio & Gallart 2004).

This paper is organized as follows. In Section 2, the method is presented. In Sections 3–6, the IAC-pop code self-consistency, error sources, and reliability of solutions are discussed under different input assumptions. In Section 7, a brief "manual" for IAC-pop execution is given. Finally, in Section 8 some final remarks are made and the main conclusions are summarized.

2. IAC-pop: A METHOD TO SOLVE THE STAR FORMATION HISTORY

2.1. Basic Definitions

The SFH is composed by several pieces of information. The rate at which stars form as a function of time (SFR) and the metallicity distribution of those stars, also a function of time (CEL), are the most important characteristics. The IMF and the binarity of stars are also related to the SFH (see Aparicio 2002). For simplicity we will adopt here the following approach: considering that time and metallicity are the most important variables in the problem, we define the SFH as a function $\psi(t, z)$ such that $\psi(t, z)dtdz$ is the number of stars formed at time t' in the interval $t < t' \leqslant t + dt$ and with metallicity z' in the interval $z < z' \leqslant z + dz$, per unit time and metallicity. $\psi(t, z)$ is a distribution function and can be identified with the usual SFR, but as a function of both time and metallicity.

There are several other functions and parameters related to the SFH that we will consider here as auxiliary. The aforementioned IMF, $\phi(m)$, and a function accounting for the frequency and relative mass distribution of binary stars, $\beta(f, q)$, are the main ones. The solution found for the SFH depends on the assumptions made for $\phi(m)$ and $\beta(f, q)$. In the most general case, they should be free and solved together with the SFH. In practice, the amount of available information may not be sufficient to attempt such an assumption-free solution, but, in any case, several choices of both $\phi(t)$ and $\beta(f, q)$ should be tried.

Other parameters affecting the solution of $\psi(t, z)$ are distance and reddening, including differential reddening. But the strongest limitation on the observational information is produced by the *observational effects*. These include all the factors affecting and distorting the observational material, namely, the signal-to-noise limitations, the defects of the detector, and the crowding and blending between stars. The consequences are loss of stars, changes in measured stellar colors and magnitudes, and external errors larger and more difficult to control than internal ones. A comparison of Figures 2 and 12 shows the distortion introduced by observational effects (see below). It must be kept in mind that IAC-pop does not account for the observational effects that must be considered and simulated in advance by the user into the synthetic CMDs.

In the following, we will concentrate in the determination of $\psi(t, z)$ on the understanding that all the remaining functions and parameters are externally checked and that proper assumptions are made for them.

2.2. The IAC-pop Methodology in Short

The procedure used by IAC-pop is based on the one introduced independently by Aparicio et al. (1997) and Dolphin (1997). Its fundamentals have been adopted and extended by several groups since then (see Section 1). The method is based on the following steps.

1. The synthetic CMD computation code IAC-star or any other code intended for the same purpose is used to generate a single global synthetic stellar population with a large number of stars with ages and metallicities following some convenient distribution over the full interval of variation of $\psi(t, z)$ in time and metallicity. The simplest case is using a constant distribution, but other approaches would be convenient in order to better sample some age or metallicity intervals. Observational effects (crowding, blending, external errors, etc.) should be simulated in the synthetic CMD.
2. The former synthetic stars are distributed in an array of partial or simple models (see Figure 3). Each contains the stars within small intervals of age and metallicity. They constitute a set of $n \times m$ models with no star in common between any two of them. Arbitrary stellar populations can be obtained by linear combinations with non-negative coefficients of the simple models of this set. These properties are similar to those of a base of a vectorial space. However, the simple model set cannot be defined as such because of their statistical nature and because of the fact that coefficients cannot be negative.
3. A set of boxes is defined in the CMD. In practice, several approaches are possible, including uniform and *a la carte*

grids. A uniform grid is more objective and less dependent on human criteria. An *a la carte* grid takes advantage of our knowledge of stellar evolution and allows different sampling of well- and poorly known stellar evolution phases. The approach we use here is a bit more sophisticated and takes advantage of the strengths of the two aforementioned approaches. Several regions, which we will call *bundles*, are defined in the CMD. Each of them is sampled by a uniform grid, but the grid bin size can be different from one bundle to another (see Figure 4).

4. An array, M_i^j, containing the number of stars from partial model i populating the CMD box j is computed. The same operation is made in the observational CMD, producing a vector, O^j, containing the number of observed stars in the box j. This step defines the parameterization of the CMD.
5. With the former information, the distribution of stars in the CMD boxes can be calculated for any model SFH as a linear combination of the M_i^j values:

$$M^j = A \sum_i \alpha_i M_i^j. \quad (1)$$

It should be noted that $\alpha_i \geqslant 0$. A is a scaling constant.

6. The SFH best matching the distribution, O^j, of the observational CMD can be found using a merit function. In particular, Mighell's χ^2_γ (Mighell 1999) is used:

$$\chi^2_\gamma = \sum_j \frac{(O^j + \min(O^j, 1) - M^j)^2}{O^j + 1}. \quad (2)$$

We will use $\chi^2_\nu = \chi^2_\gamma/\nu$, where ν is the number of freedom degrees. In our case $\nu = k - (n \times m)$, where k is the number of boxes defined in the CMD.

Minimization of χ^2_ν provides the best solution as a set of α_i values as well as a test on whether it is good enough. IAC-pop makes use of a genetic algorithm for an efficient searching of the χ^2_ν minimum. Such a procedure is required because of the large number of the problem dimensions $(n \times m)$.

7. The solution SFH can be written as

$$\psi(t, z) = A \sum_i \alpha_i \psi_i, \quad (3)$$

where ψ_i refers to partial model i, with i taking values from 1 to $n \times m$, and A is a scaling constant.

3. RUNNING IAC-pop

We have made several tests to check IAC-pop efficiency, self-consistency, solution stability, and whether it can deal with real astrophysical data. To this purpose, a synthetic stellar population has been generated with IAC-star from some arbitrary SFH. We will call this the *mock* population and denote the corresponding CMD as mCMD. The mock population is solved as if it were real data and the solution is compared with its input SFH. The IAC-star input parameters used to compute the mock population were as follows. The Teramo-BaSTI stellar evolution library (see Pietrinferni et al. 2004) and the Castelli & Kurucz (2003) bolometric correction library were used. The number of stars in the mCMD was 10^5. The star formation ranges from 14 Gyr ago to date with a constant SFR, $\psi(t)$, for that period. The metallicity increases with time, with initial and final metallicities

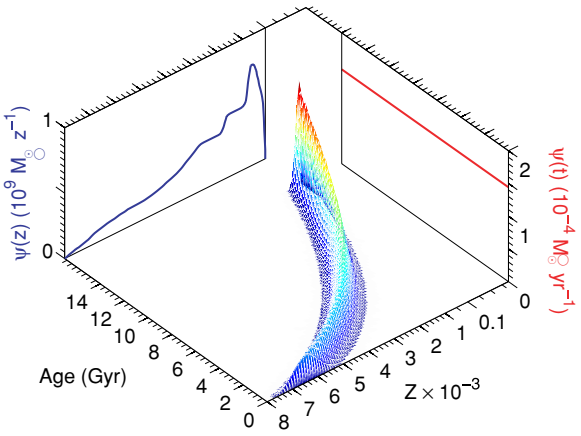

Figure 1. SFH $\psi(t, z)$ of the mock population. Age and metallicity are given in the horizontal axis. The volume below the curved surface and over the age–metallicity plane gives the mass that has been ever transformed into stars within the considered age–metallicity interval. The monodimensional $\psi(t)$ and $\psi(z)$ are shown on the ψ–age plane (red in the online version) and on the ψ–metallicity plane (blue in the online version), respectively.

(A color version of this figure is available in the online journal.)

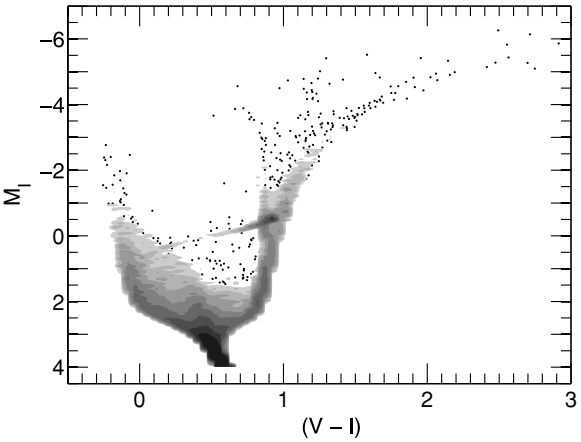

Figure 2. CMD of the mock population (mCMD). Gray levels show the density of stars. A factor of 2 in density exists between each two successive gray levels. The single dots are shown where the density is less than 8 stars per $(0.1)^2$ mag. Gray levels start respectively at 8, 16, 32, 64, 128, 256, 512, 1024, and 2048 stars per $(0.1)^2$ mag interval.

$z_0 = 0.0001$ and $z_f = 0.008$ and some metallicity dispersion at each time (see Figure 1). Finally, no binary stars were considered and the IMF by Kroupa et al. (1993) was used. The integral of $\psi(t, z)$ (i.e., the total mass ever transformed into stars) for this system is $\Psi_T = 2.02 \times 10^6\, M_\odot$.

The SFH $\psi(t, z)$ of the mock population is shown in Figure 1. The volume below the curved surface and over the age–metallicity plane gives the mass that has been ever transformed into stars within any considered age–metallicity interval. The SFRs as a function of time only, $\psi(t)$, and of metallicity only, $\psi(z)$, are also shown. The mCMD is shown in Figure 2.

According to Section 2.2, item (1), a global synthetic population has been computed as the starting point for the solution searching. We will call its CMD, sCMD. Binary stars, IMF, and stellar evolution and bolometric correction libraries used are the same as for the mock population. A constant SFR, $\psi(t, z)$, was used for the full age (from 0 to 14 Gyr) and metallicity (from 0.0001 to 0.008) ranges. The sCMD contains 3×10^7 stars. The SFH of this population is shown in Figure 3. Age and metallicity

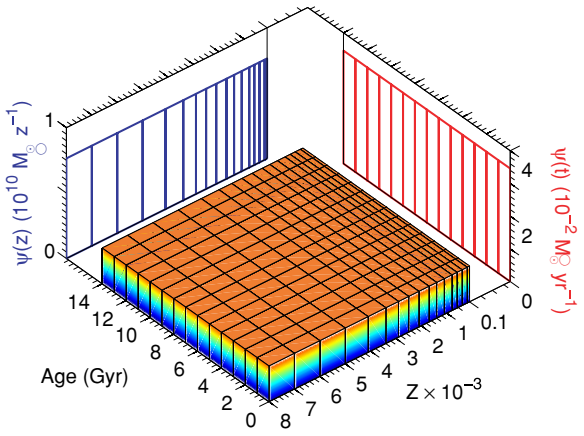

Figure 3. SFH of the global synthetic population associated with sCMD. The caption is the same as in Figure 1. The bars show the simple populations in which the global one has been divided for the analysis of the problem. See the text for details.

(A color version of this figure is available in the online journal.)

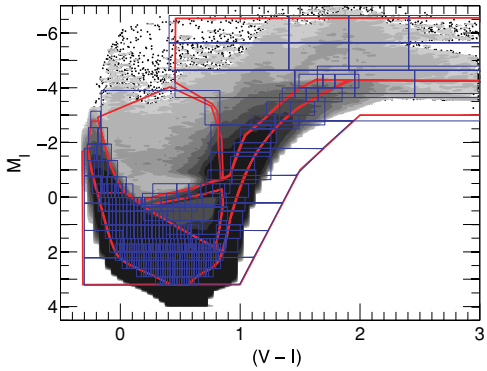

Figure 4. CMD of the global synthetic stellar population (sCMD). Gray levels show the density of stars as in Figure 2. Bundles (red in the online version) and one of the used box distributions (blue in the online version) are shown.

(A color version of this figure is available in the online journal.)

have been divided into 14 and 16 intervals, respectively. These intervals define one of the simple population sets that have been used for the solution searching, as mentioned in Section 2.2, item (2). The sCMD is shown in Figure 4.

As mentioned in Section 2.2, item (3), several bundles have been defined onto the mCMD and the sCMD. Each one has been sampled by grids of different box sizes, which depend on the CMD region or bundle. Grids are thinner in regions where age and metallicity resolution are better, like the main sequence (MS), and coarser in regions in which the distribution of stars strongly depends on poorly known parameters, like the RGB or the horizontal branch (HB). The number of boxes in a grid ranges from one to several hundreds depending on the CMD region. Figure 4 shows the bundles and one of the used box distributions, overplotted on the sCMD.

The particular box distribution used and the division of the global synthetic population in several simple populations as a function of which the solution is searched may introduce some bias and binning effects on such solution. In order to minimize them, several sets of grids and simple populations have been used. Each one is defined by shifting the set with respect to the initial one. In particular, in our case, bundles were fixed, and a total of three grid sets and 40 partial model sets were used and a solution computed for each one. The average of all of them is adopted as the final solution. Our many tests have disclosed that

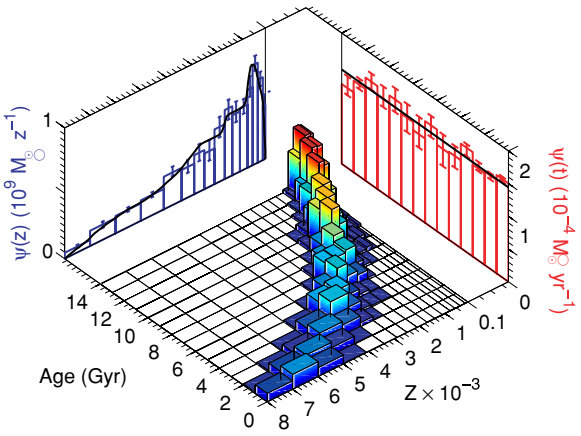

Figure 5. Solution of $\psi(t, z)$ obtained for the mock population. No observational errors have been simulated. It is the average of 120 single solutions found using the *several solutions* procedure described in the text. The caption is the same as in Figure 1. Projection of the solution onto the $\psi(t)$–age and $\psi(z)$–Z planes, obtained as integration of $\psi(t, z)$ over metallicity and time, respectively, are also shown. The monodimensional input $\psi(t)$ and $\psi(z)$ are shown by solid lines (see Figure 1). Error bars have been obtained applying the *several solutions* procedure.

(A color version of this figure is available in the online journal.)

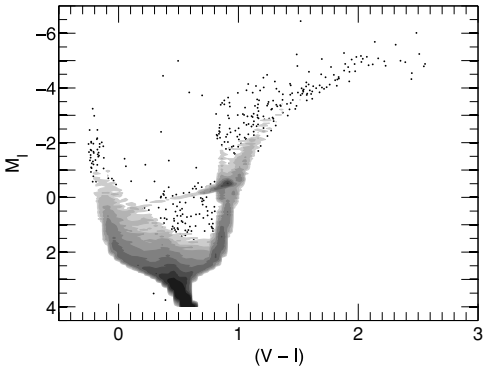

Figure 6. The CMD corresponding to the SFH shown in Figure 5 (to be compared with the mCMD shown in Figure 2).

this procedure provides very stable solutions and the best way to estimate errors (see Section 4).

A set of routines called MinnIAC is used to control the full computation process. The MinnIAC input consists of a set of parameters that define (1) the bundles to be used in the CMDs; (2) the grid size in each bundle; (3) the number of different grids to be used and the shifts to be applied to define them; (4) the division of the global synthetic population into simple populations; (5) the number of different input sets of simple populations and the shifts to be applied to define them. For each set, MinnIAC counts stars in the grids of the observational and simple population's CMDs and generates an input parameter file for IAC-pop. Once all the solutions have been obtained, MinnIAC averages them and computes errors for each age and metallicity interval as the root mean square of the solutions. MinnIAC will be provided under request but should be used at user's risk, since no support can be provided by the authors at this moment.

Figure 5 shows the $\psi(t, z)$ solution for the mock population given in Figure 1. Comparison between input and solution is simpler for the monodimensional $\psi(t)$ and $\psi(z)$ functions, also shown in Figure 5. Agreement is good, being the differences between input and solution within the error bars (see the discussion of error computation in the next section). As a further

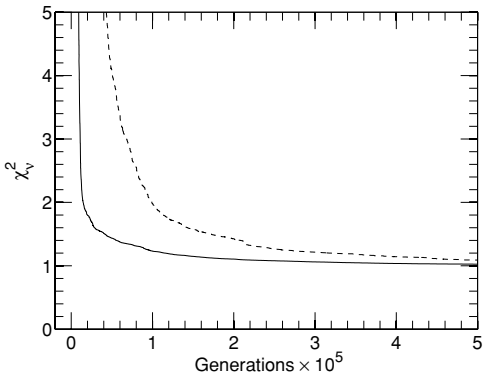

Figure 7. χ^2_ν as a function of the number of IAC-pop genetic generations. The latter is proportional to the computing time. The dashed and solid lines show χ^2_ν for two different selections of input values of genes, size of the population, and mutation rate, which are internal parameters of the genetic algorithm.

visual test, Figure 6 shows the CMD corresponding to the solution shown in Figure 5. It is to be compared with the input mCMD shown in Figure 2.

As mentioned, IAC-pop uses a genetic algorithm to look for the set of positive or null α_i parameters minimizing the χ^2_ν function given in Section 2.2, item (6). The convergence velocity depends on the choice of input parameters for the genetic code (see Charbonneau 1995). Figure 7 shows the evolution of χ^2_ν as a function of generation for our test case. The dashed and solid lines show the χ^2_ν for two different selections of input values of genes, number of individuals, and mutation rate of IAC-pop. Both inputs get almost the same χ^2_ν if the number of generations is large enough. In other words, changes in the genetic input values do not affect the final solution if the number of generations is large, but computation time, which is proportional to the number of generations, may be large if the parameter choice is not good.

4. ERROR SOURCES

Providing reliable error estimates is fundamental for the solution's meaningfulness. In principle, we can identify three kinds of error sources in the problem of retrieving the SFH from a CMD. The first one is that of internal errors, inherent to the numerical problem or related to the parameterization, i.e., the way in which bundles, grids, and also partial models are selected. The second one is that associated with observational effects (crowding, blending, etc.). They blur the CMD, distorting the information provided by it. Observational effects must be simulated in the global synthetic CMD before parameterizing it. Also, any estimate of errors of the first kind will include the observational effects. Finally, an additional uncertainty source is related to our limited knowledge of stellar evolution theory. It is difficult to test this, but using different stellar evolution libraries will produce somewhat different solutions for the same input observational data. Differences between these solutions provide a representation of this kind of uncertainty. In the following, we will discuss each of the former kinds of error sources.

4.1. Errors of the Solution

Calculating the internal error of the best solution for the SFH is not straightforward. The χ^2 test allows computing 1σ errors of the solution parameters (see Bevington & Robinson 2003; Arndt & MacGregor 1966). But this works only for Gaussian random variables. The fact that the SFH problem can depart

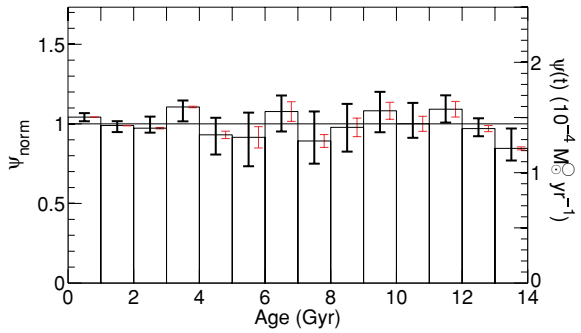

Figure 8. The projection onto the $\psi(t)$–age of the solution for the SFH given in Figure 5 is shown. The horizontal line corresponds to the input $\psi(t)$. Thick error bars have been obtained applying the *several solutions* procedure described in the text. In this case, 24 solutions have been used. Thin (red in the online version of the paper) error bars result from the *Poisson statistics* formal error computation. See the text for details.

(A color version of this figure is available in the online journal.)

significantly from Gaussian makes this approach unuseful for our purposes, as we have checked in several examples not shown here for brevity.

Errors related to the data sampling can be calculated assuming that the number of stars in each CMD box behaves according to a Poisson statistics. We will call this the *Poisson statistics* criterion. Errors are computed as follows. Once the best solution has been found, the input observational data, i.e., the number of stars in each grid box, are randomly modified according to a Poisson statistics. The best solution for the new data set is computed. This procedure is repeated several times, providing a set of solutions, the average of which is expected to be similar to the best original one. Also, if n_r such solutions have been obtained and solution r is given by the set $\alpha_{r,i}$, then

$$\sigma_{\alpha_i} = \left(\frac{\sum_r (\alpha_{r,i} - \alpha_i)^2}{n_r - 1} \right)^{1/2} \quad (4)$$

can be used as an estimate of the errors affecting α_i arising from data sampling. These errors are provided by IAC-pop. Upward and downward error bars can be obtained using only the subsets $\alpha_{r,i} \geqslant \alpha_i$ and $\alpha_{r,i} \leqslant \alpha_i$, respectively, and are also provided by IAC-pop.

The former criterion does not include all error sources and it will likely produce error underestimates. In particular, it does not take into account the effects introduced by the CMD parameterization through bundles and grids nor those related to the division of the global synthetic CMD into partial models. A simple way to evaluate these errors is using the dispersion of the 120 solutions computed and explained in Section 3. This is the procedure used in this paper. We will see below that it is a good estimate of all the internal error sources. For brevity, we will call this the *several solutions* criterion. The error bars shown in all the figures have been calculated in this way. It is time consuming, but we think it is necessary if a stable solution and a realistic estimate of errors are sought. The routine MinnIAC delivers the errors computed in this way (see Section 3).

Figure 8 shows the input and solution $\psi(t)$ together with the error obtained by the *several solutions* (thick, black error bars) and the *Poisson statistics* (thin, red error bars) criteria. That the latter are underestimates of total errors should be clear from the fact that in 12 out of 14 intervals differences between solution and input are larger than the error bars and, in several cases, much larger than three times that. However,

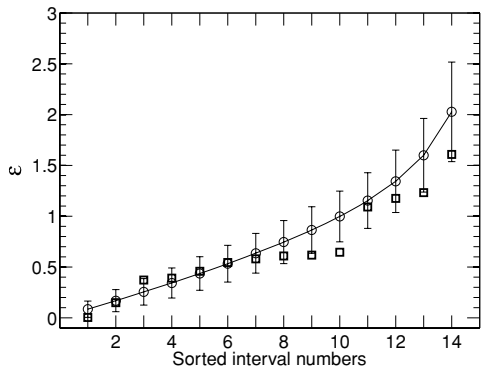

Figure 9. ϵ parameter is represented as a function of age interval order number, after sorting by increasing values of ϵ. The parameter is defined as $\epsilon_i = |\psi_i^{\rm out}(t) - \psi_i^{\rm in}(t)|/\sigma_i$ where i stands for the age interval and $\psi_i^{\rm out}(t)$ and $\psi_i^{\rm in}(t)$ refer to the output (or solution) and input values of $\psi(t)$, respectively. In other words, ϵ parameters are the absolute values of the differences between solution and input measured in units of the corresponding σ values. The thick squares show the values of the solution given in Figures 5 and 8. The thin circles and the line connecting them show the behavior of a normalized Gaussian random variable. 10^5 experiments in which 14 values are randomly selected have been done to obtain this. The circles show the averages of the 10^5 experiments and error bars give their rms dispersions.

this does not seem to be the case for the errors computed by the *several solutions* criterion. To test if the errors obtained in this way are similar to what should be expected in a Gaussian case the following test has been done. For each age interval, the parameter $\epsilon_i = |\psi_i^{\rm out}(t) - \psi_i^{\rm in}(t)|/\sigma_i$ has been computed, where i stands for the age interval, σ_i is the rms of the solutions, and $\psi_i^{\rm out}(t)$ and $\psi_i^{\rm in}(t)$ refer to the output (or solution) and input values of $\psi(t)$, respectively. In other words, ϵ parameters are the absolute values of the differences between solution and input measured in units of the corresponding σ values. The ϵ parameters have been sorted and plotted in Figure 9 together with the values of a standard Gaussian random variable. For the latter, 10^5 experiments have been done. For each one, 14 values have been randomly given to the random variable and then sorted from smaller to larger. The values represented in Figure 9 (open circles) are the averages for the 10^5 experiments while the errors bars show the corresponding rms dispersions. It can be seen that a reasonable agreement exists between our results and the Gaussian case, indicating that the *several solutions* approach produces reliable estimates of total internal errors.

4.2. Including Observational Effects

Observational effects include limited signal-to-noise, incompleteness, source blending, image read-out noise as well as not fully removed artifacts in the data reduction process (flat-field correction, etc.). All together, their effects on the CMD are the loss of stars and dispersion and shift of points, all depending on magnitude and color.

The best way to test how all these effects influence the SFH solution is working with synthetic CMDs, in which they have been simulated. For our particular purpose we have introduced random rejection and Gaussian dispersion of points, both depending on magnitude, in the mCMD and the sCMD. This approach is enough for this test although a more realistic simulation of observational effects should be used in real cases (see Hidalgo et al. 2009). For rejection, we have used the completeness curve obtained for the CMD of the Phoenix dwarf galaxy (Hidalgo et al. 2009) and displayed in Figure 10. This curve shows the probability that a star of magnitude I is conserved

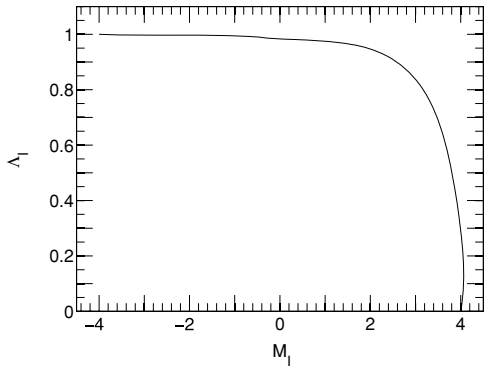

Figure 10. Function used to simulate incompleteness in mCMD and sCMD. The fraction of remaining stars (Λ_I) is given as a function of I. Values 1 and 0 mean that all or none stars remain, respectively.

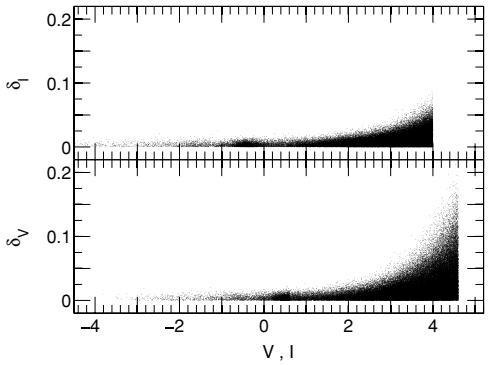

Figure 11. Shifts applied to the magnitudes in the mCMD and sCMD to simulate data dispersion.

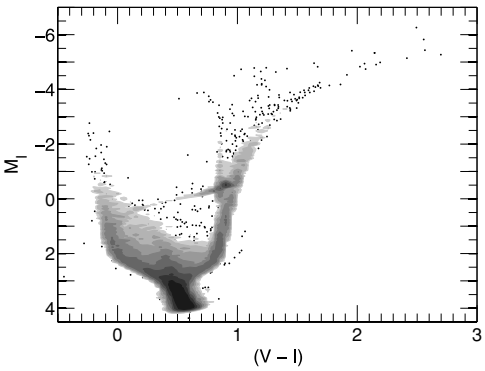

Figure 12. CMD of the mock population after simulating observational errors in it. The figure legends are the same as in Figure 2.

in mCMD or sCMD. A shift in δV and δI magnitudes is then applied to conserved stars. δV and δI are decided stochastically according to Gaussian distributions of σ_V and σ_I which are functions of V and I, respectively, and have been estimated using the CMD of the Phoenix dwarf galaxy (Hidalgo et al. 2009). Figure 11 shows the δV and δI actually used. Figure 12 shows mCMD after simulation of the observational effects.

Figure 13 shows the solution after simulating observational effects in mCMD and sCMD. Figure 14 shows the CMD corresponding to the SFH given in Figure 13. As a result of the effects introduced in the CMD, $\psi(t, z)$ and also the projected $\psi(t)$ and $\psi(z)$ appear noisier than for the observational effect free case. However, results are similar to those of the observational effects free case, showing IAC-pop robustness against observational effects.

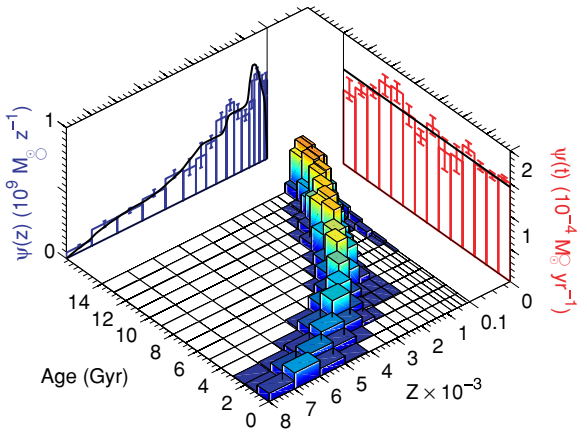

Figure 13. Solution of $\psi(t, z)$ obtained for the mock population with observational effects simulated. It is the average of 120 single solutions found using the *several solutions* procedure described in the text. The input monodimensional $\psi(t)$ and $\psi(z)$ are shown by solid black lines. Error bars have been obtained applying the *several solutions* procedure. As a consequence of the observational effects, solutions appear noisier than for the observational effect free case shown in Figure 5.

(A color version of this figure is available in the online journal.)

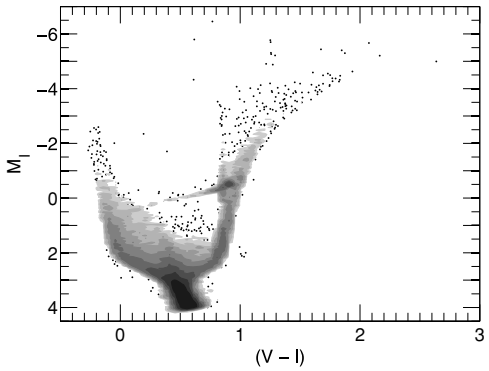

Figure 14. CMD corresponding to the solution SFH shown in Figure 13. To be compared with the mCMD shown in Figure 12.

4.3. The Effects of Different Stellar Evolution Libraries Predictions

Working on CMDs in which observational effects have been simulated allows testing the capability of IAC-pop to handle real observations. However, sCMD and mCMD have been built with the same stellar evolution library, which removes the uncertainty introduced by our limited knowledge of stellar evolution. An idea of how this modeling affects results can be obtained by using different libraries to generate mCMD and sCMD. To this purpose, IAC-star has been used to compute an sCMD using the Padua stellar evolution library (Bertelli et al. 1994). The input parameters have been the same as before. Figure 15 shows the corresponding solution. Discrepancies between input and solution show now significant systematic effects. Differences are attributed to the stellar evolution model differences and therefore the use of more than one stellar evolution library is recommended when analyzing a real population to test these effects.

Table 1 summarizes the tests carried out in the present section. Column 1 identifies the test. Column 2 gives the χ^2_ν value of the solution obtained for each test. Columns 3, 4, and 5 give, respectively, the total mass (M_T), mean age ($\langle$age$\rangle$), and mean metallicity ($\langle z\rangle$) of the stars in the mock population (first row)

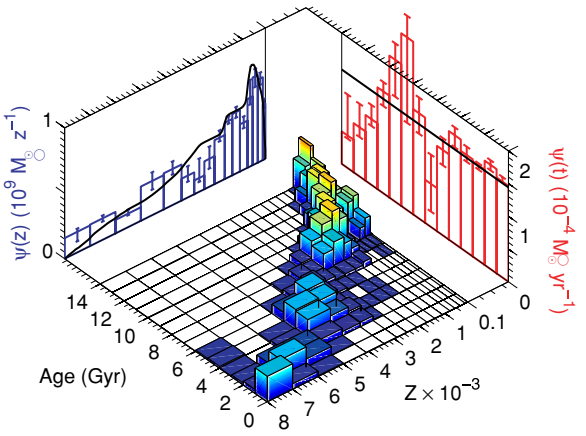

Figure 15. Solution using different stellar evolution libraries to compute sCMD and mCMD. It is the average of 120 single solutions found using the *several solutions* procedure described in the text. The Teramo-BaSTI (Pietrinferni et al. 2004) library is used to compute the mock population (mCMD) and the Padua one (Bertelli et al. 1994) for the global synthetic one (sCMD). Error bars have been obtained applying the *several solutions* procedure.

(A color version of this figure is available in the online journal.)

Table 1
Results for the Self-Consistency Test

CMD	χ^2_ν	M_T (10^6 $M_\odot$)	$\langle$age$\rangle$ (Gyr)	$\langle z\rangle$
Mock CMD		2.02	7.00	0.0026
No observ. effects	1.1	2.00 ± 0.02	6.9 ± 1.1	0.0026 ± 0.0005
With observ. effects	0.9	2.00 ± 0.02	6.9 ± 1.1	0.0026 ± 0.0005
BaSTI-Padua	4.6	2.03 ± 0.03	6.7 ± 1.0	0.0030 ± 0.0006

and the solutions. Agreement on integral and average values between mock population and solutions is good in all the cases, but χ^2_ν is large for the case in which different stellar evolution libraries are used to compute the mock and the global synthetic populations.

5. A FURTHER TEST: SHARP BURSTS AND TIME RESOLUTION

Time resolution is an important issue in the solution of the SFH. In general, it worsens for older ages. Moreover, it is ultimately limited by the quality of the data—which depends on the signal to noise with which each feature in the CMD is observed, the spatial resolution of the data, and the number of stars in the CMD—but not by the choice of the temporal sampling, which can be arbitrarily small. Olsen (1999), in his Figure 10, shows how the solution found for a synthetic stellar population is closer to the input as time sampling intervals become larger. This indicates that solutions averaged over large time intervals may be quite accurate, but that short time sampling could result in spuriously fluctuating solutions as also shown in Aparicio et al. (1997) (see also Skillman & Gallart 2002).

To test both time resolution and accuracy, a mock population in which star formation has proceeded in sharp bursts has been solved. To this purpose the mock population shown in Figure 16 has been used together with the Teramo-BaSTI (Pietrinferni et al. 2004) library to compute the mCMD of Figure 17 in which observational effects have been simulated. A solution has been sought using a sCMD computed from the global synthetic population shown in Figure 3 and the Teramo-BaSTI library also, following the same procedure explained above.

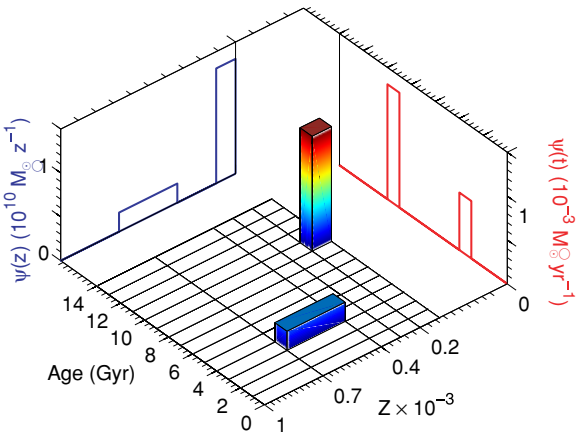

Figure 16. Mock stellar population composed by two narrow bursts used to test IAC-pop time resolution and precision.

(A color version of this figure is available in the online journal.)

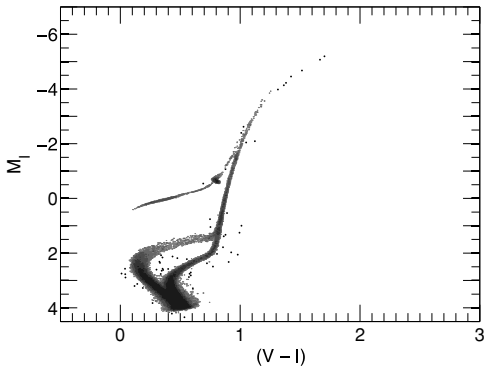

Figure 17. mCMD corresponding to the SFH shown in Figure 16. Observational effects have been included.

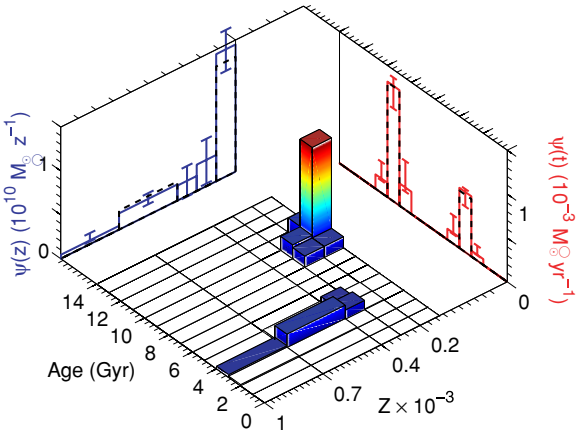

Figure 18. IAC-pop solution of $\psi(t, z)$ for the mock population shown in Figure 16. It is the average of 120 single solutions found using the *several solutions* procedure described in the text. The Teramo-BaSTI (Pietrinferni et al. 2004) library has been used to compute the mock and global synthetic populations. The dotted lines in the monodimensional representations $\psi(t)$ and $\psi(Z)$ show the input functions. Error bars have been obtained applying the *several solutions* procedure.

(A color version of this figure is available in the online journal.)

The solution is shown in Figure 18. The solution accuracy and precision are good, which provide a further test of internal consistency of IAC-pop, now including its capability to recover age and burst sharpness, at least for the time resolution and observational effects used in our example.

6. GENERALIZING IAC-pop

IAC-pop has been designed with the idea in mind of solving for $\psi(t, z)$. However, the code, as it is, is blind to the nature of the parameters behind the models used to generate the input information provided to it. Rigorously, the code searches for the linear combination (with positive or null coefficients) of a set of l reference vectors best reproducing a set of k properties of a template vector of dimension k. If run for solving the SFH, the latter is associated with the stellar population, k is the number of bins in which the CMD is divided, and $l = n \times m$ is the number of simple populations into which the global synthetic sCMD has been divided. We have discussed the SFH case in detail, but it should be kept in mind that the code is of more general application and that, if the l reference vectors are defined otherwise, the found solution will include other properties of the galaxy or, in general, of the problem being analyzed.

7. IAC-pop MANUAL

IAC-pop is made available for free use. It can be downloaded from the Internet site http://iac-star.iac.es/iac-pop. Together with IAC-pop, a number of interactive software facilities will also be made available from this site or from sites accessible from it, including the synthetic stellar populations and CMD generator IAC-star. IAC-pop is currently offered for several computer operating systems, such as Linux, MacOS, or Windows. In the following, we will describe the input parameters and summarize the content of the output file.

7.1. Input Data

The input is provided in two files. The first one, which we call the input parameter file, provides several choices about the computation procedure as follows.

1. The input and output data files (see below).
2. The number of age and metallicity bins, n and m.
3. The number of boxes, k, defined in the observational and synthetic CMDs.
4. A seed for the random number generator used by the genetic algorithm.
5. The number of computed solutions, i.e., the number of times that the genetic algorithm is run. Each run starts with a different random number generator seed and provides an independent solution. In this way, the possibility that the genetic code is trapped in a secondary minimum is minimized (see Charbonneau 1995).
6. The number of generations computed for each single genetic solution.
7. The number of solutions changing input star count values according to a Poisson statistics. This provides a way of formal error estimation based upon the internal accuracy of the input observational data. This step is quite time consuming and should be set to 0 when not necessary.
8. A good enough χ^2_ν value. The program will accept as good enough a solution with a χ^2_ν less or equal to this even if it has not reached the number of generations provided above. To switch off this condition, set this value to 0.

The second file, which we call the input data file, is a list of $(l + 1) \times k$ numbers. For more clarity we can assume them organized as $l + 1$ rows each one containing k numbers, but it must be noted that separation into different rows is not necessary. The content of the rows is as follows.

1. First row: observational data. The k values provide the number of stars in each of the k boxes defined in the CMD for the observational data. For a general problem, they provide the values of the evaluated property.
2. Rows from second to last (i.e., $(l+1)$): data for the simple synthetic populations. Explicitly, the ith row provides the number of stars in each of the k boxes defined in the CMD of the $(i-1)$th simple population extracted from the global synthetic population. For a general problem, they provide values corresponding to the $(i-1)$th simple model.

In other words, each row contains the star counts in the boxes defined in the observational (first row) and the simple synthetic population (second to last rows) CMDs. Note that the k boxes are the same for all the involved CMDs, observational and synthetic, and that the latter should contain a simulation of observational effects. The boxes set definition and the time and metallicity resolution are to be decided by the user. For simplicity, in the following we will refer only to the case of interest in this paper of solving a SFH using CMDs, but it should be kept in mind that any other, similarly parameterized problem could be faced.

7.2. Output File

Upon completion, IAC-pop produces an output file containing the solutions and the formal errors. The content of the output file is structured in several labeled sets with the following content.

1. The solutions obtained in the several independent code runs. Each row corresponds to one solution and contains $l+1$ data: the l α_i parameters of the solutions plus its χ^2_ν value.
2. The best of the former solutions, i.e., the solution having the $\chi^2_{\nu,\min}$ value.
3. The average of the former solutions and their dispersions. This average could in some cases be preferable to the solution having the $\chi^2_{\nu,\min}$ value as it smooths out possible no realistic fluctuations. The dispersions are indicative of the solution stability, but not of its actual error.
4. Dispersions of the computed solutions around the best one and the number of solutions found above and below the best one. This information is complementary to evaluate solution stability and fluctuations.
5. Formal error estimate. Solutions found for several observational input data sets in which the star counts corresponding to each of the k boxes defined in the CMD are randomly changed according to a Poisson statistics within $\sqrt{n}_j$, where n_j is the actual number of stars in the box j. It must be noted that these errors are underestimates of the total internal errors.
6. Standard deviations of the former solutions. Upward and downward error bars and number of solutions above and below the best one are obtained in the same way as above.

8. FINAL REMARKS AND CONCLUSIONS

Summarizing, IAC-pop is a program designed to solve the SFH of a complex stellar population system, like a galaxy, from the analysis of the CMD. To this purpose, IAC-pop uses a genetic algorithm (Charbonneau 1995) to minimize a reduced Mighell's, χ^2_ν, merit function (Mighell 1999) obtained from comparison of the parameterization of an observed and a synthetic CMD. The code main characteristics can be sketched as follows.

1. The code needs the computation of only a single global synthetic CMD. As many simple population model CMDs as necessary are later extracted from it. We call this sCMD initial global synthetic CMD.
2. It is designed to solve simultaneously for age and metallicity distributions, i.e., for the star formation rate as a function of time and metallicity, which also provides the chemical enrichment law.
3. The parameterization of observed and synthetic CMDs is done by dividing the CMDs in several boxes and counting out the stars in each one. This is the information provided to the code.
4. The former implies that the code application is not restricted to solve the problem of the SFH, but it is of general application to problems in which a similar parameterization can be done.
5. It is important to note that observational effects (crowding, blending, completeness, etc.) must be simulated in the synthetic global data or in the input parameterization prior to running the IAC-pop.
6. A genetic algorithm is used to minimize the aforementioned merit function χ^2_ν.
7. The final solution is provided as a linear combination of positive or null coefficients of the input simple population models.
8. In its current version, IAC-pop provides the best solution for one or several runs. It also provides a formal error estimate based on Poissonian random fluctuations of the input. It should be noted that these formal errors seem to be underestimates of the total internal errors of the problem. More realistic error estimates are obtained as the dispersion of several solutions obtained with several input parameterization to IAC-pop (which we have named *several solutions* procedure). The IAC-pop user is strongly encouraged to implement it. The routine MinnIAC will be provided under request to help in this job.

IAC-pop has been run through several consistency tests. To this purpose a mock stellar population has been computed using IAC-star and analyzed with IAC-pop to obtain its SFH as if it were a real one. Results have been compared with the input used to compute the mock population under different assumptions.

1. For the first test, an SFH continuously varying as a function of time and metallicity was used for the mock population. The test simply consisted in deriving the SFH in an observational error free scenario and using a global sCMD computed with the same stellar evolution library as for the mock population. Results were in quite good agreement with input, proving the IAC-pop code internal consistency.
2. The second test was a repetition of the former but after simulating observational effects both in the mock population mCMD and the global sCMD. Although noisier, the resulting SFH was also in good agreement with the input SFH, showing the robustness of the method against realistic observational effects.
3. The third test was a repetition of the former, including observational effects, but using different stellar evolution libraries to compute the mock population mCMD and the global sCMD. This is expected to reproduce the effects introduced in the solution by the inaccurate knowledge of the stellar evolution physics. Systematic trends show up due to the differences in the stellar evolution models, and therefore the use of more than one stellar evolution library is recommended when analyzing a real population to control these effects.
4. Finally, the fourth test is done on a mock population made of two sharp bursts at young and intermediate to old ages.

The bursts are well reproduced, even if observational effects are simulated, if the same stellar evolution library is used to compute the mock population mCMD and the global sCMD.

In summary, IAC-pop has been shown to be a useful tool to obtain the SFH from the CMD of resolved stellar systems. The program can be downloaded from the site http://iac-star.iac.es/iac-pop, with the only requirement of referencing this paper and acknowledging the IAC in any derived publication. The routine MinnIAC is also offered under request and at user's risk. Its use also requires referencing this paper. It is intended to produce further improved versions of the program after feedback by the user community.

Developing IAC-pop and MinnIAC has been greatly benefited from long discussions maintained with and many tests performed by S. Cassisi, C. Gallart, M. Monnelli, and E. Skillman and by the very interesting comments of the anonymous referee. The authors are funded by the IAC (grant 310394) and by the Science and Technology Ministry of the Kingdom of Spain (grants AYA2004-3E4104 and AYA2007-3E3507).

REFERENCES

Aparicio, A. 2002, in ASP Conf. Ser. 274, Observed HR Diagrams and Stellar Evolution Models: The Interplay Between Observational Constraints and Theoretical Limitations, ed. T. Lejeune & J. Fernandes (San Francisco, CA: ASP), 429
Aparicio, A., Carrera, R., & Martínez-Delgado, D. 2001, AJ, 122, 2524
Aparicio, A., & Gallart, C. 2004, AJ, 128, 1465
Aparicio, A., Gallart, C., & Bertelli, G. 1997, AJ, 114, 669
Aparicio, A., Tikhonov, N., & Karachentsev, I. 2000, AJ, 119, 177
Arndt, R. A., & MacGregor, M. H. 1966, Methods Comp. Phys., 6, 253
Baade, W. 1944, ApJ, 100, 137
Bertelli, G., Bressan, A., Chiosi, C., Fagotto, F., & Nasi, E. 1994, A&AS, 106, 275
Bertelli, G., Mateo, M., Chiosi, C., & Bressan, A. 1992, ApJ, 388, 400
Bevington, P. R., & Robinson, D. K. 2003, Data Reduction and Error Analysis for the Physical Sciences (3rd ed., New York: McGraw-Hill)
Castelli, F., & Kurucz, R. L. 2004, in IAU Symp. 210, Modelling of Stellar Atmospheres, ed. N. Piskunov, W. W. Weiss, & D. F. Gray (San Francisco, CA: ASP), A20
Charbonneau, P. 1995, ApJS, 101, 309
Chiosi, E., & Vallenari, A. 2007, A&A, 466, 165
Dolphin, A. E. 1997, New Astron., 2, 397
Dolphin, A. E. 2000a, MNRAS, 313, 281
Dolphin, A. E. 2000b, ApJ, 531, 804
Gallart, C., Aparicio, A., Bertelli, G., & Chiosi, C. 1996, AJ, 112, 1950
Gallart, C., Freedman, W. L., Aparicio, A., Bertelli, G., & Chiosi, C. 1999, AJ, 118, 2245
Harris, J., & Zaritsky, D. 2001, ApJS, 136, 25
Hernández, X., Valls-Gabaud, D., & Gilmore, G. 1999, MNRAS, 304, 705
Hidalgo, S. L., Aparicio, A., Martínez-Delgado, D., & Gallart, C. 2009, ApJ, submitted
Holtzman, J. A., Smith, G. H., & Grillmair, C. 2000, AJ, 120, 3060
Holtzman, J. A., et al. 1999, AJ, 118, 2262
Kroupa, P., Tout, C. A., & Gilmore, G. 1993, MNRAS, 262, 545
Mighell, K. J. 1999, ApJ, 518, 380
Olsen, K. A. G. 1999, AJ, 117, 2244
Pietrinferni, A., Cassisi, S., Salaris, M., & Castelli, F. 2004, ApJ, 612, 168
Rizzi, L., Held, E. V., Bertelli, G., & Saviane, I. 2003, ApJ, 589, L85
Sabbi, E., et al. 2007, AJ, 133, 44
Skillman, E., & Gallart, C. 2002, in ASP Conf. Proc. 274, Observed HR Diagrams and Stellar Evolution, ed. T. Lejeune & J. Fernandes (San Francisco, CA: ASP), 535
Tolstoy, E., & Saha, A. 1996, ApJ, 462, 672
Tosi, M., Greggio, L., Marconi, G., & Focardi, P. 1991, AJ, 102, 951
Vergely, J.-L., Köppen, J., Egret, D., & Bienaymé, O. 2002, A&A, 390, 917
Wyder, T. K. 2001, AJ, 122, 2490